Advantages of in vivo measurement of human skin thermal conductance using a calorimetric sensor

Pedro Jesús Rodríguez de Rivera[1] · Miriam Rodríguez de Rivera[1] · Fabiola Socorro[1] · Jose A. L. Calbet[2,3] · Manuel Rodríguez de Rivera[1]

Abstract

Thermal conductivity of the skin has been measured by in vivo procedures since the 1950s. These devices usually consist of temperature sensors and heating elements. In vivo measurement of skin thermal conductivity entails several difficulties. It is necessary to adequately characterize the excitation produced by the measurement. In addition, the thermal penetration depth of each instrument is different. These factors have led to the development of a multitude of techniques to measure the thermal conductivity or related magnitudes such as thermal conductance. In our case, we have built a calorimetric sensor designed to measure this magnitude directly and non-invasively. The device implements the basic principles of calorimetry and is capable of characterizing the thermal magnitudes of a 2×2 (4) cm^2 skin region. The sensor consists of a measuring thermopile with a thermostat cooled by Peltier effect. Several skin measurements performed under different conditions resulted in a thermal conductance ranging from 0.017 to 0.050 WK^{-1}. This magnitude, measured in vivo, is different in each studied area and depends on several factors, such as physical activity and the physiological state of the subject. This new sensor is a useful tool for studying the human body thermoregulatory response.

Keywords Direct calorimetry · Medical calorimetry · Skin heat loss · Skin thermal properties · Thermal conductance

Introduction

Human body's heat dissipation is of great interest in physiology. Human body temperature regulation depends on surface heat dissipation. This heat loss is controlled by systems that act in coordination, such as sweating, vasoconstriction, or vasodilation. The human body's heat dissipation is highly variable. For example, during physical activity, dissipation can increase from 3.8 to 77 mWcm^{-2}. Currently, indirect calorimetry is often used to assess the metabolic rate of the human body at rest [1, 2] or during physical activity [3, 4].

Indirect calorimetry consists of relating the volumes of O$_2$ absorbed and CO$_2$ released with the heat generation of the human body by empirical expressions. Heat flow can also be locally measured on specific areas of the human body, by using different contact sensors, mainly heat flow sensors.

Contact sensors have also been developed to measure thermal properties of the skin such as thermal diffusivity, specific heat capacity, or thermal conductivity. Knowledge of the human body's thermal properties is also of great interest. Several in vitro measurements have been performed using different procedures [5, 6]. However, in vivo measurement is particularly problematic, as it involves studying a control volume that is not fully defined.

In this work we will focus on the in vivo measurement of thermal conductance in localized areas of the human skin. Thermal conductance is a macroscopic magnitude that defines the amount of energy dissipated by a given skin area, and depends directly on thermal conductivity. Thermal conductivity measurements have been performed for more than 60 years. Generally, to obtain a property that relates the heat dissipation change with the temperature change, it is necessary to simultaneously measure the

✉ Manuel Rodríguez de Rivera
    manuel.rguezderivera@ulpgc.es

1 Department of Physics, University of Las Palmas de Gran Canaria, Las Palmas de Gran Canaria, Spain

2 Department of Physical Education and Research Institute of Biomedical and Health Sciences (IUIBS), University of Las Palmas de Gran Canaria, Las Palmas de Gran Canaria, Spain

3 Department of Physical Performance, The Norwegian School of Sport Sciences, Oslo, Norway

variation of these two quantities. For this reason, measuring devices usually consist of temperature sensors and heating systems. This is the basis of most instruments, although there are methods based on digital thermography [7] or zero-heat-flux (ZHF) thermometry. As a consequence of the growing interest in this field, several novel procedures have been developed in recent years. In 2016, *Grenier E,* et al. [8] studied the effects of compression stockings on cutaneous microcirculation by assessing skin thermal conductivity. In 2018, Wang et al. [9] studied the phenomena of vasoconstriction and vasodilation at different room temperatures by assessing skin thermal resistance. For this purpose, they used heat flow sensors and applied modeling of the tissue under study. Likewise, *Okabe T,* et al. [10] measured thermal conductivity in different areas of the skin using a power pulse technique. Using the same instrument, later in 2019, Okabe et al. performed measurements on cancerous tissue [11].

This paper presents a calorimetric sensor for the measurement of the thermal conductance (in WK^{-1}) of a 2×2 (4) cm^2 area of skin. This sensor has two important advantages: (1) the direct and non-invasive measurement of the skin thermal conductance, (2) incorporates a programmable thermostat that allows to control the thermal disturbance of the sensor on the skin, allowing the detailed study of the heat transfer phenomenon by conduction between the human body and the thermostat of the sensor.

The order of this work is as follows. First, a brief description of the experimental system and the measurement and calculation methods of the skin thermal conductance is given. Next, results from two experiments are presented: (1) on different areas of the skin with subjects at rest and (2) on the inner thigh area with subjects performing a physical activity. The practical utility of the sensor for assessing the degree of vasoconstriction or vasodilatation of a localized region of skin, especially during intense physical activity, is demonstrated. Finally, our results are compared with those of other authors.

The calorimetric sensor

The calorimetric sensor consists of a measurement thermopile placed between a programmable thermostat and an aluminum plate. This aluminum plate is in contact with the skin when the sensor is applied on the human body. The thermostat is made of aluminum and contains an RTD sensor (resistance temperature detector) and a heating resistor. The cooling system is based on a Peltier element, a heatsink, and a fan. Calibration and operation of the sensor are detailed in previous work [12, 13]. Figure 1 shows the calorimetric sensor applied on the thigh and the temple. In the first case (Fig. 1a), the sensor is applied manually. In the second case (Fig. 1b), an adapted attachment is used.

The experimental system includes a calibration base which has two functions: (1) to calibrate and verify the sensor operation and (2) to provide the initial sensor baseline. A triple power supply (E3631A by Agilent) powers the Peltier element, the thermostat heating resistor, and the calibration base resistor. A data acquisition system (34970A with 34901A by Agilent) reads the calorimetric signal and the ambient, skin, thermostat, and calibration base temperatures. Both instruments are connected to a laptop via GPIB bus (82357B by Agilent). The acquisition and control program is written in Microsoft Visual C + + and the sampling period is 0.5 s. In steady state, the oscillation of the signal provided by the measuring thermopile is ± 0.2 mV, the oscillation of the thermostat temperature is ± 5 mK, and the oscillation of the thermostat power is ± 5 mW. Thus, the uncertainty of the power measured by the sensor is ± 5 mW [12–14].

Thermal conductance measurement methods

This calorimetric sensor was initially developed for measuring the heat dissipation of the skin as a function of the sensor's thermostat temperature. To determine the heat dissipation, an error minimization method is used (MatLab fminsearch function [15]). In the calculation, we consider

Fig. 1 Calorimetric sensor placed on **a** thigh and **b** temple
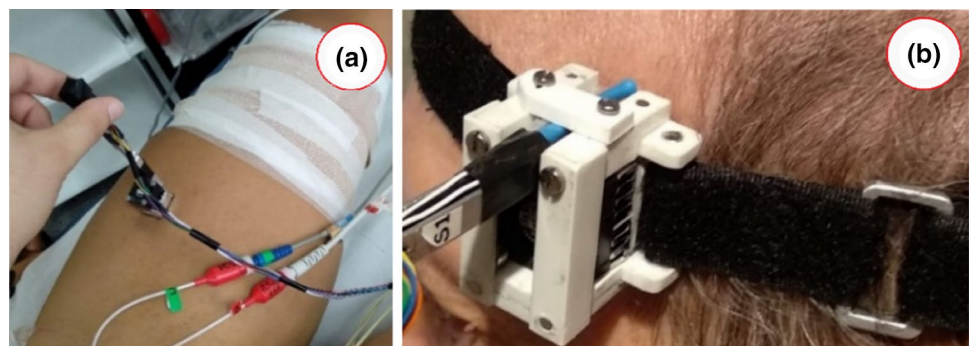
that the heat dissipation is defined by a power function (W) that takes into account the stationary power values for each temperature of the thermostat and the transient caused by the instantaneous contact between the sensor and the skin [13]. The calculation method determines the parameters of the power function (W) that provide the minimum error in the reconstruction of the calorimetric signal [12, 13]. For this reconstruction, we use a model that relates the heat power through the sensor (W) and the power dissipated in the sensor thermostat (W_{ther}) with the calorimetric signal (y) and the thermostat temperature (T_{ther}). Equation 1 relates these variables in steady state with corrected baselines.

$$\begin{pmatrix} \Delta y \\ \Delta T_{ther} \end{pmatrix} = \begin{pmatrix} K_{11} & K_{12} \\ K_{21} & K_{22} \end{pmatrix} \begin{pmatrix} \Delta W \\ \Delta W_{ther} \end{pmatrix}. \tag{1}$$

The sensitivity matrix is determined from calibration measurements: $K_{11} = 109.4$ mVW^{-1}, $K_{12} = -56.12$ mVW^{-1}, $K_{21} = 9.15$KW^{-1}, and $K_{22} = 12.00$ KW^{-1} [15].

Figure 2 shows the heat dissipation, the thermostat power, and calorimetric signal of three consecutive measurements, for constant sensor thermostat temperatures of 28, 32, and 36 °C. Each of the measurements in Fig. 2 is performed by the same procedure. The sensor is initially on its calibration base, and when steady state is reached, it is applied to the skin, keeping the thermostat temperature constant. When the calorimetric signal reaches steady state on the skin, the sensor is placed back on the calibration base. In the heat dissipation graph, two power peaks can be observed. These

peaks are a consequence of the instant application of the sensor on the skin and the relocation of the sensor on its base. In the measurements shown, the sensor was manually held on the skin (Fig. 1a), and the baseline corresponds to the location of the sensor on its calibration base.

The calorimetric sensor can be operated in different ways by varying the thermostat temperature setting. See for example, the result is shown in Fig. 2: depending on the sensor's thermostat temperature, the skin reacts emitting different dissipations. Due to this feature of the sensor, we can measure the thermal conductance by different methods. The four methods used until now are described below.

1) As we can see in Fig. 2, as the temperature of the thermostat increases, the skin dissipation decreases. The relationship between the sensor thermostat temperature change (ΔT) and the skin heat dissipation change (ΔW) allows the definition of a thermal conductance ($\Delta W/\Delta T$) of the skin region affected by the measurement (4 cm^2). The procedure initially developed required at least three successive measurements of heat dissipation, with a total duration of one hour [14].

2) However, making several successive measurements has disadvantages due to the sensor movement and the time required for the measurement. Therefore, a new method was proposed, in which the sensor remains on the skin while the temperature of the sensor thermostat changes [12]. This procedure reduces the time required to 15 min, in a single application to the skin.
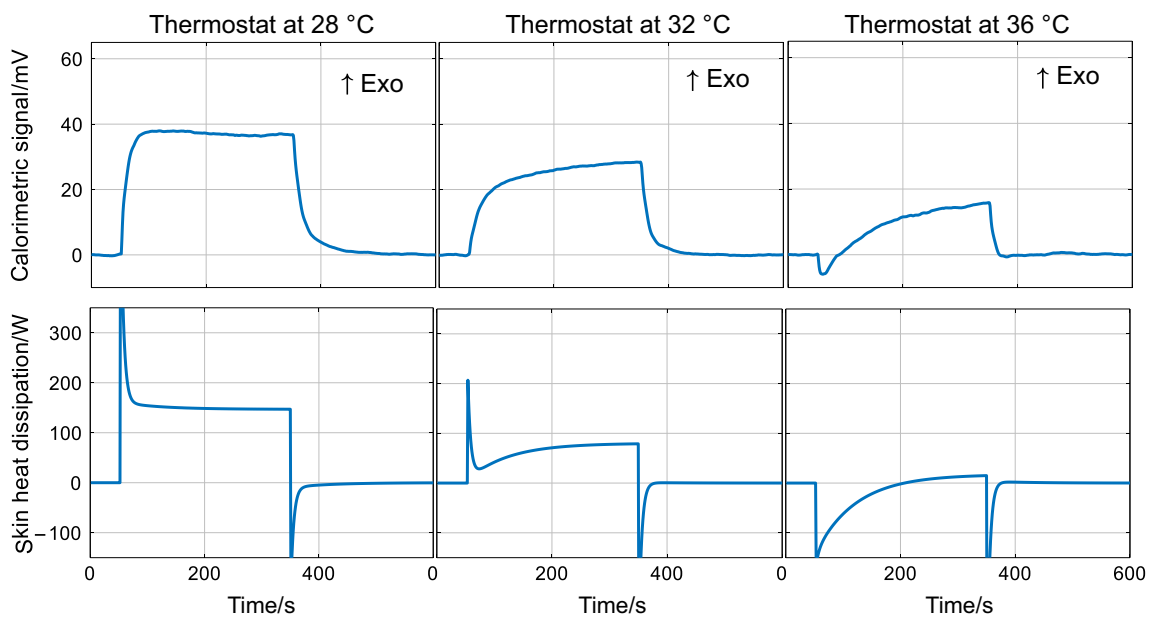

Fig. 2 Calorimetric signal, thermostat power, and heat dissipation of the skin, in three consecutive measurements at different sensor thermostat temperatures of 28, 32, and 36 °C. Baselines have been corrected

Figure 3 shows an example of this type of measurement. The calorimetric signal, the thermostat temperature, and the calculated dissipation are shown. In this case, the thermostat temperature changes from 26 to 36 °C (at 4 Kmin^{-1}) while the sensor is placed on the skin. Before and after the application of the sensor on the skin, the sensor is located on the calibration base, so the baseline corresponds to the situation of the sensor on its calibration base. In this measurement, the sensor was manually held on the skin (Fig. 1a).

3) Another method consists of holding the sensor on the skin with an adapted strap (Fig. 1b) during the entire measurement. The advantage of this procedure is that the initial and final baselines correspond to situations where the sensor is on the skin. The disadvantage is that it is not possible to calculate the heat dissipation in absolute value; only its variation can be calculated.

In other words, this procedure allows to determine the variation of the heat dissipation ($W_1 - W_2$) as a function of the variation of the thermostat temperature ($T_1 - T_2$). As a consequence, it allows to determine the thermal conductance of the skin area where the sensor is applied. This method requires more time of the sensor on the skin (25 min) but provides better results. An example of this type of measurement is shown in Fig. 4. When the sensor reaches the thermal equilibrium with the skin, a variation of the thermostat temperature is programmed. In this case, the thermostat temperature varies linearly from 28 to 37 °C (at 3 Kmin^{-1}), and when it reaches steady state at 37 °C, it returns to the original temperature of 28 °C at the same rate.

The ratio between the heat dissipation change and the thermostat temperature change defines a thermal conductance P, which is a combination of the sensor conductance ($P_S \approx 0.1$ WK^{-1}) and the tissue conductance (P_{body}). To determine the thermal conductance, only the stationary values of heat dissipation and thermostat temperature are needed. Equation 2 shows this measurement principle, which is common to the methods mentioned above.

$$P = \left| \frac{W_2 - W_1}{T_2 - T_1} \right| = \frac{1}{1/P_S + 1/P_{body}} \; ; \quad T_2 - T_1 = \Delta T_{ther}.$$
(2)

In this equation W_1 and W_2 are the steady-state heat powers corresponding to the thermostat temperatures T_1 and T_2. In these measurement methods, all the reference temperatures (T_1 and T_2) are in the sensor itself (in our case, in the thermostat). For this reason, we could classify these methods as Sensor Temperature Referenced Methods (T_{sensor} *Referenced Methods*). Some authors employ similar procedures, using instruments that emit controlled dissipations and measure the temperature; being the dissipations stationary [16, 17], sinusoidal (3ω method) [18], or pulsed [10, 11]. Similarly, other authors use instruments that control temperature and measure power [11].

4) However, other authors consider that the skin heat flux is proportional to the heat flux transferred between the inside of the human body, which is at a temperature T_{core}, and the skin, which is at a temperature T_{skin} [9, 19]. In this case, a heat flux sensor is used, and the tem-
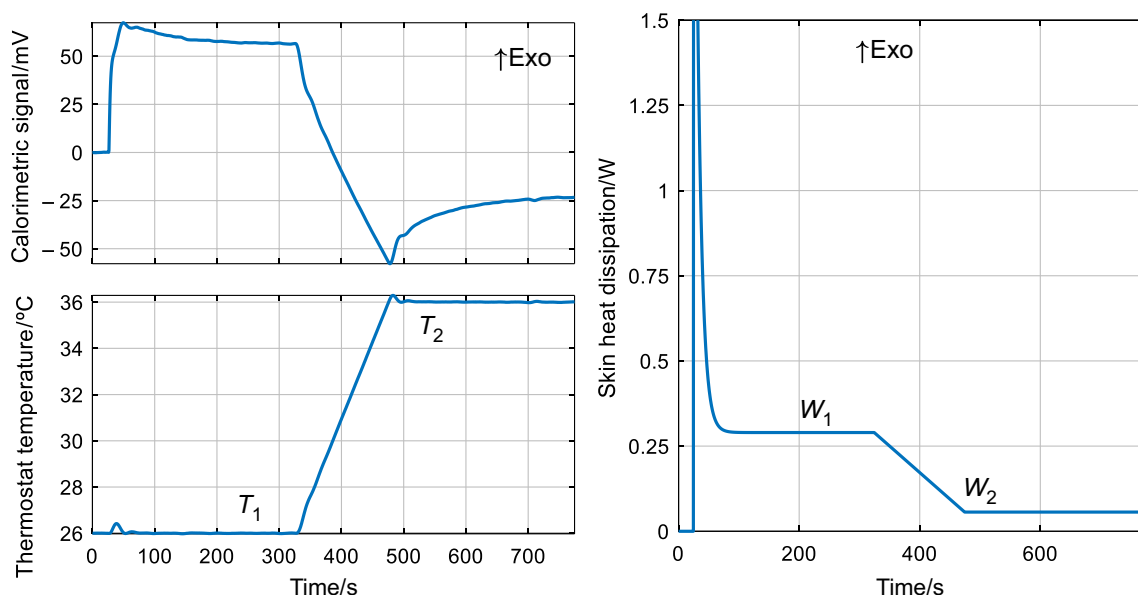

Fig. 3 Calorimetric signal, sensor's thermostat temperature, and heat dissipation. Measurement on the skin carried out by programming a linear variation of the thermostat temperature
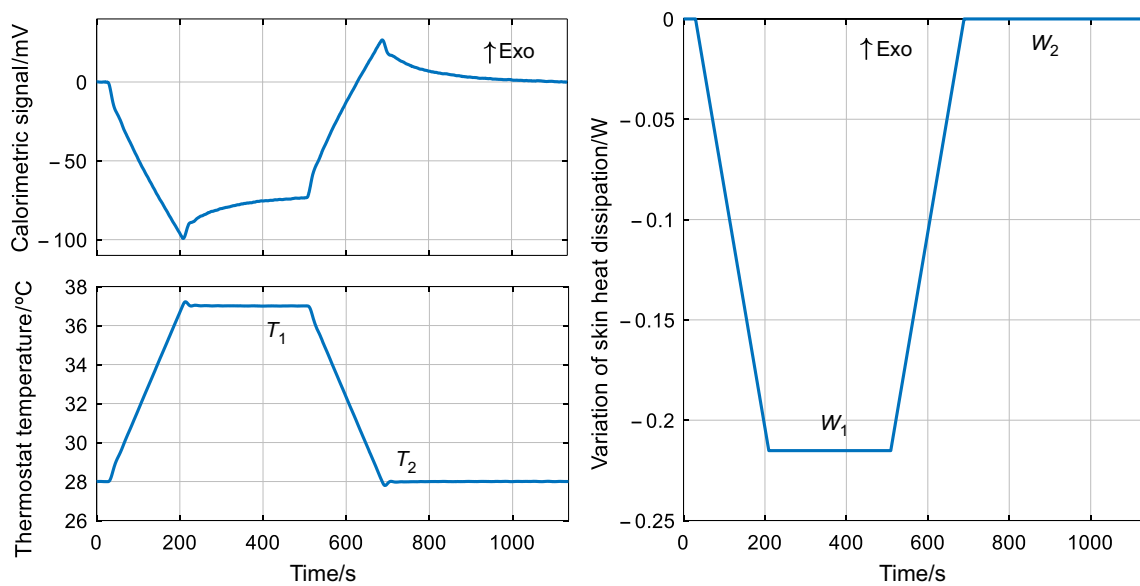
Fig. 4 Calorimetric signal, sensor thermostat temperature, and heat dissipation variation. Measurement carried out by programming a linear variation of the thermostat temperature, with an adapted strap

perature difference (skin—core) is obtained externally. These methods consider the T_{skin} and T_{core} temperatures as a reference. We can define these methods as T_{core} *Referenced Methods*, since one of the references is set at the internal temperature of the human body. With our calorimetric sensor, we can apply this method, using the thermostat temperature and the human body internal temperature obtained with an additional sensor, as reference. With a measurement similar to those shown in Fig. 2, and the knowledge of T_{core}, the thermal conductance P would be calculated as follows:

$$P = \frac{W}{T_{\text{ther}} - T_{\text{core}}} = \frac{1}{1/P_{\text{S}} + 1/P_{\text{body}}} \tag{3}$$

where W is the heat dissipation measured at the thermostat temperature T_{ther}. Equations 2 and 3 are different ways to determine a thermal conductance between the heat source (human body) and the sensor's thermostat, and the values obtained with each equation are similar. Both equations involve the assumption of steady state of the skin area. This thermal conductance is of great utility in practice, since a change in this thermal conductance is usually associated with the degree of vasodilatation or vasoconstriction in the area of skin where the measurement is performed.

Results

Two measurement campaigns have been carried out with the calorimetric sensor. These campaigns correspond to different procedures and objectives. In total, sixteen subjects participated in these experiments, of which anthropometric characteristics are shown in Table 1.

Six subjects participated in the first campaign (1–6 in Table 1). The objective of the campaign was to study the thermal conductance in different areas of the human body at rest. For this purpose, a variation of the sensor's thermostat temperature was programmed while it was applied to the skin (Figs. 2 and 3). Ten subjects participated in the second campaign (7–16 in Table 1). The objectives were to study the variation of thermal conductance in the inner thigh area before and after physical exercise, and to

Table 1 Anthropometric characteristics of the subjects who participated in the studies: age (years), mass (kg), height (m), and sex (M: male, F: female)

Subject	1	2	3	4	5	6	7	8	9	10	11	12	13	14	15	16
Age/years	62	29	27	57	31	24	25	23	25	24	20	21	21	23	20	29
Mass/kg	71	68	83	68	74	53	–	72	76	79	80	–	54	54	74	88
Height/m	1.60	1.72	1.77	1.66	1.49	1.61	–	1.68	1.81	1.72	1.68	–	1.60	1.55	1.68	1.69
Sex	M	M	M	F	F	F	M	M	M	M	M	F	F	F	F	F

study the performance of the sensor by applying a T_{core} *Referenced Method*. The T_{core} temperature is determined by inserting a thermistor into the subject's femoral artery as described elsewhere [20].

First measurement experiment: rest

In the first campaign, method 2) was used, explained in Sect. 3. Some measurements have been reproduced with method 3), resulting in similar values. Measurements were made on six areas of the human body: temple, hand, abdomen, thigh, heel, wrist and sternum. Subjects were resting seated. Temperature and humidity conditions were controlled: $T_{room} = 23.5$ °C and 55% RH. Sensor thermostat temperatures were $T_1 = 26$ ºC and $T_2 = 36$ ºC. Table 2 shows the average thermal conductance results obtained with Eq. 1.

Thermal conductance varied between 0.017 and 0.050 WK^{-1}. The mean value was 0.024 WK^{-1} at the heel, 0.032 WK^{-1} at the hand, 0.022 WK^{-1} at the thigh, 0.029 WK^{-1} at the abdomen and temple, and 0.040 WK^{-1} at the wrist. The lowest values were measured at the heel, and the highest at the wrist. The standard deviation was on average 7%. Zones with lower conductance correspond to regions with higher fat percentage, and zones with higher conductance are regions with greater blood supply and thinner subcutaneous adipose tissue. Each zone has a characteristic conductance, although the differences between subjects are equally marked. For example, the conductance obtained in the abdomen for each of the six subjects was 0.029, 0.025, 0.031, 0.029, 0.024, 0.034 WK^{-1}, respectively. These measurements were made for a thermostat temperature increase of 10 K at a rate of 4 Kmin^{-1}.

Additionally, several measurements were performed on the wrist of subject 1, applying different increments of the thermostat temperature of 2.5, 5.0, 7.0, and 9.0 K. Figure 5 shows the variation of thermal conductance in these cases. Measurements were also made for different heating/cooling rates (1, 2, and 3 Kmin^{-1}). These experiments demonstrated that the measured thermal conductance does
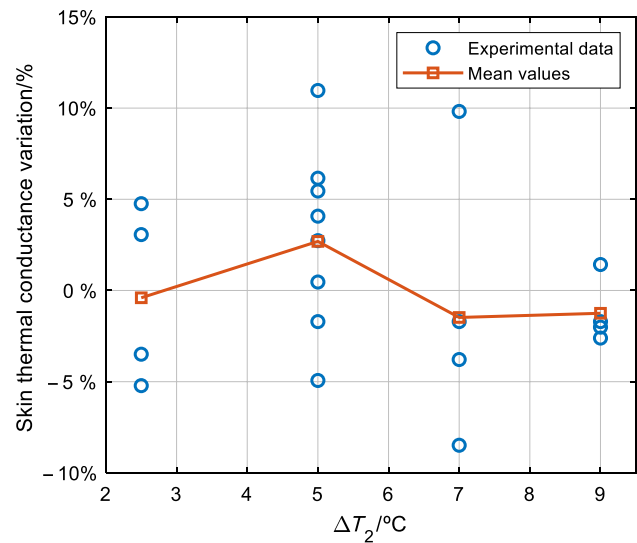

Fig. 5 Thermal conductance variation as a function of thermostat temperature increase (ΔT_{ther}). Measurements performed in the volar area of the left wrist of subject 1

not depend on the increase or the rate of thermostat temperature change.

Second measurement experiment: exercise

In the second campaign, the measurements were performed with the thermostat at $T_{ther} = 28$ ºC. This temperature is chosen because the steady state is reached earlier (Fig. 2). Knowing the steady-state heat dissipation W, the thermal conductance of the skin is determined with Eq. 3. The ambient conditions varied between 20 and 28 °C. However, the ambient temperature was practically constant during each measurement, given its short duration (≈ 10 min). The procedure for these measurements was as follows:

– A thermistor is surgically inserted into the subject's femoral artery to measure blood temperature during the experiment (Fig. 1a).

Table 2 Thermal conductance (in WK^{-1}) in the first experiment (rest), subjects 1 to 6 of Table 1. Results obtained varying the temperature of the sensor thermostat (Eq. 2). Mean $\pm$ standard deviation (%) values are shown

Subject	Temple	Hand	Abdomen	Thigh	Heel	Wrist
1	0.033 $\pm$ 8%	0.035 $\pm$ 5%	0.029 $\pm$ 4%	0.023 $\pm$ 7%	0.024 $\pm$ 3%	0.037 $\pm$ 9%
2	0.028 $\pm$ 5%	0.030 $\pm$ 10%	0.025 $\pm$ 7%	0.022 $\pm$ 5%	0.022 $\pm$ 7%	–
3	0.035 $\pm$ 9%	0.030 $\pm$ 6%	0.031 $\pm$ 6%	0.024 $\pm$ 5%	0.026 $\pm$ 6%	0.043 $\pm$ 7%
4	0.028 $\pm$ 10%	0.036 $\pm$ 18%	0.029 $\pm$ 4%	0.023 $\pm$ 13%	0.028 $\pm$ 1%	–
5	0.027 $\pm$ 7%	0.028 $\pm$ 5%	0.024 $\pm$ 13%	0.019 $\pm$ 8%	0.023 $\pm$ 5%	–
6	0.031 $\pm$ 6%	0.033 $\pm$ 16%	0.034 $\pm$ 9%	0.021 $\pm$ 11%	0.024 $\pm$ 8%	–
Mean $\pm$ SD	**0.029 $\pm$ 8%**	**0.032 $\pm$ 10%**	**0.029 $\pm$ 8%**	**0.022 $\pm$ 8%**	**0.024 $\pm$ 5%**	**0.040 $\pm$ 8%**

- After a rest time, the subject begins an incremental exercise on a cycloergometer. This exercise lasts 20–30 min. Then, the subject rests in supine position for 90 min.
- Finally, the subject remains at rest and the thermistor is removed. To avoid excessive blood flow, the protocol involves compression on the puncture site which almost impedes the blood flow for 20 min after removal of the thermistor (occlusion). After the release of the compression, some reactive hyperemia is observed as reflected by the reddish color of the skin which lasts few minutes.

Table 3 shows the mean thermal conductance obtained at different times of the experiment. It can be seen that the mean value of these results is of the same order of magnitude as the results obtained with the method of the first campaign at the same location. However, there are differences, which may be due to both the method itself and the conditions of the experiment. It is also remarkable for the high variability of this method, and the average standard deviation is greater than 27%. Authors using a similar method, such as Brajkovic et al. [19], also often obtain results with high variability. Wang et al. [9] attribute this uncertainty to the oversimplicity of the model. We agree with this hypothesis: using a single heat flux value, the accuracy of the thermal conductance obtained is limited by the oscillation of the heat flux. Previous work has shown that heat flux can fluctuate between 10 and 24% in subjects sitting at rest under the same environmental conditions [14]. Therefore, we conclude that it is necessary to review the modeling when using the Tcore Referenced Method to determine the thermal conductance of the skin.

In the experiments conducted, we can highlight some observations. Shortly after physical exercise (2–5 min), thermal conductance increases by 30% compared to the resting value. As time elapses, thermal conductance slowly decreases. At the end of the resting time and after the occlusion of the blood flow, hyperemia occurs, and the thermal conductance increases by 15%. After completion of the occlusion, the thermal conductance returns to a value close to the pre-procedure value. These observations are consistent with vasodilatation in the tissues when exercise is performed, and with the accumulation of blood in the skin when circulation is occluded.

Discussion

Since the 1950s, attempts have been made to measure the thermal conductivity of skin in vivo [16]. Thermal conductivity, λ (in $WK^{-1} m^{-1}$), is the most commonly used thermal quantity by authors to characterize skin. Other authors use the thermal resistance per unit area, r (in $KW^{-1} m^2$) [9, 19]. We use the thermal conductance P (in WK^{-1}) because it is the quantity directly measured by the calorimetric sensor. There is an equivalence between these quantities, which depends on the geometry of the heat-affected zone. Considering a prismatic geometry of surface (A) and thermal penetration depth (d), we can relate these quantities with the following simplified expression:

$$P = \frac{W_{body}}{\Delta T} = \lambda \frac{A}{d} = \frac{A}{r} \tag{4}$$

In general, the area of the tissue under study (A) is known. However, the thermal penetration depth (d) is not initially known. Different magnitudes can only be compared when the geometry of the heat-affected zone or the thermal penetration depth is known. Some authors calculate this parameter in different ways. Van de Staak et al. carried out a study of the thermal penetration depth by measurement on inert solids [16] using Burton's method. In this way, he obtained a relationship between the thickness of the solid used and the

Table 3 Thermal conductance in the thigh (in WK^{-1}) in the second experiment (exercise), subjects 7–16 in Table 1. Result obtained with Eq. 3

Subject	At rest	After exercise 5–10 min	After exercise 20–60 min	After exercise 80–90 min	While occlusion	After occlusion
7	0.024	0.028	0.027	–	–	–
8	0.016	0.025	0.024	0.023	0.027	0.022
9	0.016	0.024	0.025	0.022	0.028	0.024
10	0.018	0.029	0.031	0.030	–	–
11	0.026	0.018	0.020	0.016	–	–
12	0.025	0.028	0.030	–	–	–
13	0.008	0.013	0.015	0.014	0.018	0.018
14	0.015	0.023	0.023	0.026	0.030	0.024
15	0.014	0.016	0.020	0.019	0.022	0.021
16	0.011	0.013	0.016	0.012	0.014	0.014
Mean ± SD	**0.017 ± 34%**	**0.022 ± 28%**	**0.023 ± 24%**	**0.020 ± 31%**	**0.023 ± 27%**	**0.020 ± 20%**

percentage of thermal conductivity measured with his conductivity meter. He obtained an exponential curve, a function of distance, of which length constant is 0.6 mm. Webb et al. obtained a depth of 0.5 mm [17] using the expression of Silas [21], and Tian et al. obtained a maximum depth of 0.1 mm [18] using the expression of David [22]. On the other hand, Okabe et al. define the thermal penetration depth as the depth at which the temperature increases more than 0.1 K [10], obtaining a value of 0.9 mm. In our case, in order to express our results in units of thermal conductivity, we consider a prismatic heat-affected zone of 4 cm2 and 4 mm thermal penetration depth. This depth is determined from the heat capacity measurement [12] and contrasted using the Silas expression [21].

Figure 6 shows the thermal conductivity λ calculated from the thermal conductance obtained with our calorimetric sensor, and those obtained by other authors, in each area of the human body at rest. Each point corresponds to a mean value and the line through it to its standard deviation. The rectangles define the maximum and minimum measured values. The wide range indicates the large variability of the thermal conductivity of the skin, which makes it difficult to study and understand. These results show the normal range of this thermal property. As a reference to these measurements, we can highlight that the thermal conductivity measured in vitro is 0.17 to 0.24 $Wm^{-1} K^{-1}$ for fat, 0.28 to 0.36 $Wm^{-1} K^{-1}$ for cortical bone, 0.32 to 0.50 $Wm^{-1} K^{-1}$ for skin, and 0.48 to 0.56 $Wm^{-1} K^{-1}$ for blood [23].
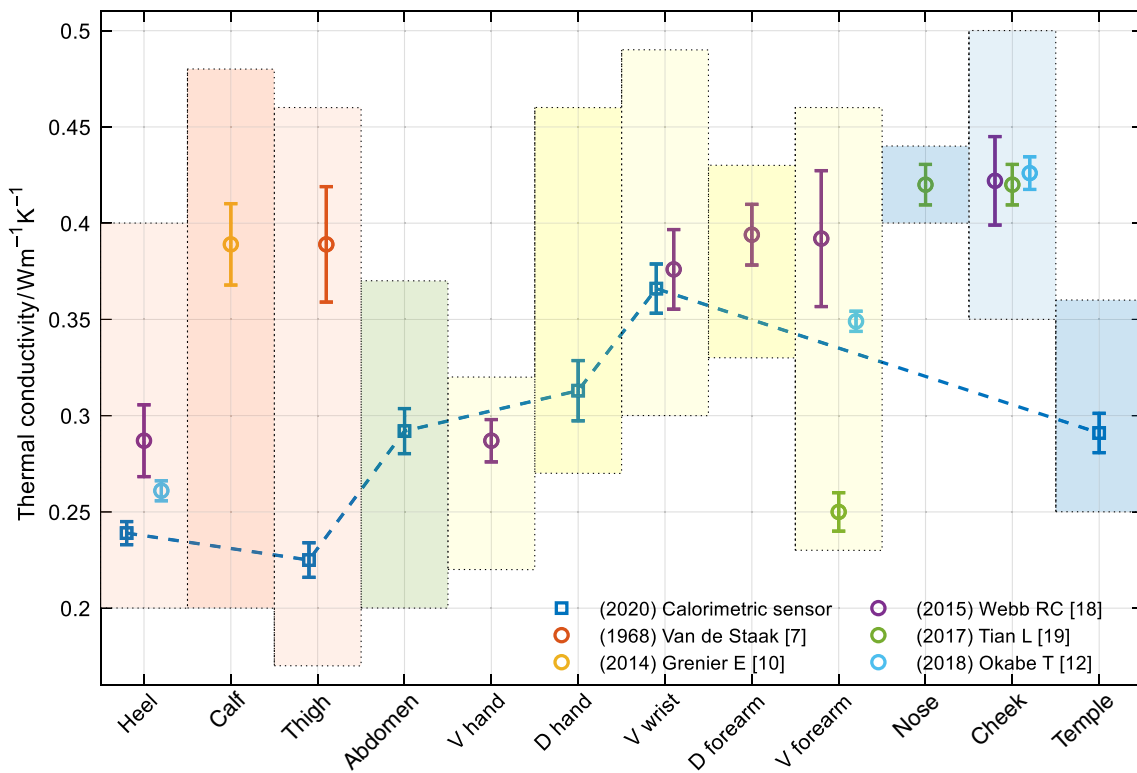

Fig. 6 Thermal conductivity (λ) measured in vivo in different areas of the human body, by different authors, while subjects are at rest

Table 4 Measurement conditions of Fig. 6. Author, sensor used, year, number of subjects (n), T_{room}, thermal penetration depth (d), and area of the sensor (A)

Author	Sensor	year	n	T_{room} °C	d mm	A mm^2
van de Staak WJBM [16]	Ring flat conductivity meter	1968	102	25.0	0.6	88
Grenier E [8]	Hematron	2014	30	22.0	–	254
Webb RC [17]	Ultrathin conformal array	2015	25	–	0.5	400
Tian L [18]	Flexible 3ω sensors	2017	2	–	0.1	600
Okabe T [10]	G-H thermistor probe	2018	5	26.0	0.9	0.30
This work	Calorimetric sensor	2021	6	23.5	3–4	400

Table 4 shows the characteristics of the measurements shown in Fig. 6: the author, the year of the work, the instrument, its thermal penetration depth, d, and its measuring surface, A, the number of subjects, and the room temperature. The procedures used in the results shown in Fig. 6 can be included in the Tsensor Referenced Methods. Although the values shown in Fig. 6 are at rest, van de Staak [16], Grenier [8], and Tian [18] performed measurements by altering the human body in different ways, by occluding blood flow, applying compression measures, or inducing urticaria, respectively.

See that there is consistency in the results shown in Fig. 6. Thermal conductivity obtained on the same skin area is similar using different instruments. Exceptions to this are the thigh and volar forearm areas. This may be due to inaccuracies in defining the area (the thigh is a large and inhomogeneous region), or perhaps to differences in the thermal penetration depth. The lowest thermal conductivity values are obtained at the heel, and the highest at the nose and cheek. The most studied locations are the cheek, the forearm, the wrist, and the heel. On the other hand, in our measurements, we observed that the difference in thermal conductivity is greater between subjects than between zones. This predominant intra-subject variability is consistent with that observed by Webb et al. [17] and Okabe et al. [10], and it is probably due to anthropometric differences between subjects.

Skin thermal conductivity can also vary depending on the environmental conditions. We observed that, for a constant room temperature, a high thermal conductance implies a higher skin temperature. Okabe et al. [10] also observed a similar correlation between thermal conductivity and skin temperature. If the ambient temperature changes, the thermal conductivity may change. Some authors have characterized these changes and related them to vasoconstriction and vasodilatation [9, 19].

Regarding physical exercise, this activity is associated with an increase in cutaneous blood circulation [24, 25], so a change in the thermal properties of the skin is predictable. This is proven in our experiment: thermal conductance increases by 27% after physical exercise. Brajkovic et al. also observed a similar variation (40%) [19].

Another phenomenon that can modify the thermal conductance of the skin is the restriction of blood flow in a limb, which can lead to a blood accumulation in the outermost layers of the skin [26]. In our experiment, we observed that, when blood flow occlusion is performed, the thermal conductance increases by 17%. Van de Staak et al. [16] applied a similar procedure and also observed an increase in thermal conductance of 8%. Other authors have carried out experiments along the same lines. Grenier et al. [8] detected an increase in thermal conductivity of 16% when applying compression stockings that promote blood circulation, and in 2017, Tian et al. [18], observed an increase in

thermal conductivity of 32% after producing urticaria on the forearm.

Conclusions

– We have developed a calorimetric sensor that consists of a thermopile equipped with a programmable thermostat. Directly measuring the skin thermal conductance with a non-invasive method is interesting to study the thermal properties of the skin and the thermoregulatory responses in humans.

– From the experiments carried out, we have found that it is more convenient to apply measurement methods in which all the temperatures used in the calculation are referenced to the sensor itself (T_{sensor} *Referenced Methods*).

– We have also experimentally verified that the thermal conductance measured with the calorimetric sensor does not depend on the amplitude of the thermostat temperature rise or on the rate of temperature change.

– One difficulty associated with contact sensors developed in the literature is the necessity to define a heat-affected zone, often by defining a thermal penetration depth of the instrument. The calorimetric sensor presented in this work is able to measure an absolute value of thermal conductance (in WK^{-1}), corresponding to an area of 4 cm^2 of skin. Therefore, it is not necessary to define a heat-affected zone to obtain a result.

– Each skin area has a different thermal conductance. At rest, this magnitude has an average standard deviation of 7%. After intense physical activity, thermal conductance increases by 27% and during hyperaemia by 15%. A change of this property is associated with the degree of vasodilatation or vasoconstriction in the skin area where the measurement is taken.

References

1. Alves VGF, Da Rocha EEM, Gonzalez MC, Fonseca RBV, Silva MHD. Resting energy expenditure measured by indirect calorimetry in obese patients: variation within different BMI ranges. J Parenter Enter Nutr. 2020. https://doi.org/10.1155/2011/534714.

2. Nakagata T, Yamada Y, Naito H. Metabolic equivalents of body weight resistance exercise with slow movement in older adults using indirect calorimetry. Appl Physiol Nutr Metab. 2019. https://doi.org/10.1139/apnm-2018-0882.

3. Speakman JR, Selman C. Physical activity and resting metabolic rate. Proc Nutr Soc. 2003. https://doi.org/10.1079/PNS2003282.

4. David NH, Ronald GT. Support of the metabolic response to burn injury. The Lancet. 2004. https://doi.org/10.1016/S0140-6736(04)16360-5.

5. Giering K, Minet O, Lamprecht I, Müller G. Review of thermal properties of biological tissues. SPIE-Int Soc Opt Eng. 1995. https://doi.org/10.1007/978-3-319-95432-5_4.

6. Wiegand N, Naumov I, Nőt LG, et al. Differential scanning calorimetric examination of pathologic scar tissues of human skin. J Therm Anal Calorim. 2013. https://doi.org/10.1007/s10973-012-2839-8.

7. Otsuka K, Okada S, Hassan M, Togawa T. Imaging of skin thermal properties with estimation of ambient radiation temperature. IEEE Eng Med Biol Mag. 2002. https://doi.org/10.1109/memb.2002.1175138.

8. Grenier E, et al. Effect of compression stockings on cutaneous microcirculation: evaluation based on measurements of the skin thermal conductivity. Phlebol/Venous Forum R Soc Med. 2016. https://doi.org/10.1177/0268355514564175.

9. Wang L, Chong D, Di Y, Yi H. A revised method to predict skin's thermal resistance. Therm Sci. 2018. https://doi.org/10.2298/TSCI1804795W.

10. Okabe T, Fujimura T, Okajima J, Aiba S, Maruyama S. Non-invasive measurement of effective thermal conductivity of human skin with a guard-heated thermistor probe. Int J Heat Mass Transf. 2018. https://doi.org/10.1016/j.ijheatmasstransfer.2018.06.039.

11. Okabe T, Fujimura T, Okajima J, et al. First-in-human clinical study of novel technique to diagnose malignant melanoma via thermal conductivity measurements. Sci Rep. 2019. https://doi.org/10.1038/s41598-019-40444-6.

12. Rodríguez de Rivera PJ, et al. A method to determine human skin heat capacity using a non-invasive calorimetric sensor. Sensors. 2020. https://doi.org/10.3390/s20123431.

13. Rodríguez de Rivera PJ, et al. Method for transient heat flux determination in human body surface using a direct calorimetry sensor. Measurement. 2019. https://doi.org/10.1016/j.measurement.2019.02.063.

14. Rodríguez de Rivera PJ, et al. Measurement of human body surface heat flux using a calorimetric sensor. J Thermal Biol. 2019. https://doi.org/10.1016/j.jtherbio.2019.02.022.

15. https://es.mathworks.com/help/matlab/ref/fminsearch.html. Accessed 12 Jan 2022..

16. Van de Staak WJBM, et al. Measurements of the thermal conductivity of the skin as an indication of skin blood flow. J Investig Dermatol. 1968. https://doi.org/10.1038/jid.1968.107.

17. Webb RC, Pielak RM, Bastien P, Ayers J, et al. Thermal transport characteristics of human skin measured in vivo using ultrathin conformal arrays of thermal sensors and actuators. PLoS ONE. 2015. https://doi.org/10.1371/journal.pone.0118131.

18. Tian L, Li Y, Webb RC, et al. Flexible and stretchable 3ω sensors for thermal characterization of human skin. Adv Func Mater. 2017. https://doi.org/10.1002/adfm.201701282.

19. Brajkovic D, et al. Cheek skin temperature and thermal resistance in active and inactive individuals during exposure to cold wind. J Therm Biol. 2004. https://doi.org/10.1016/j.jtherbio.2004.08.068.

20. Morales-Alamo D, Losa-Reyna J, Torres-Peralta R, Martin-Rincon M, Perez-Valera M, Curtelin D, Ponce-González JG, Santana A, Calbet JA. What limits performance during whole-body incremental exercise to exhaustion in humans? J Physiol. 2015. https://doi.org/10.1113/JP270487.

21. Silas EG. Transient plane source techniques for thermal conductivity and thermal diffusivity measurements of solid materials. Rev Sci Instrum. 1991. https://doi.org/10.1063/1.1142087.

22. David C. Thermal conductivity measurement from 30 to 750 K: the 3omega method. Rev Sci Instrum. 1990. https://doi.org/10.1063/1.1141498.

23. It's Foundation. https://itis.swiss/ Accesed 30 august 2021.

24. Saunders NR, Tschakovsky ME. Evidence for a rapid vasodilatory contribution to immediate hyperemia in rest-to-mild and mild-to-moderate forearm exercise transitions in humans. J Appl Physiol. 2004. https://doi.org/10.1152/japplphysiol.01284.2003.

25. Tschakovsky ME, Sheriff DD. Immediate exercise hyperemia: contributions of the muscle pump vs. rapid vasodilation. J Appl Physiol. 2004. https://doi.org/10.1152/japplphysiol.00185.2004.

26. Patterson SD, et al. Blood flow restriction exercise: considerations of methodology, application, and safety. Front Physiol. 2019. https://doi.org/10.3389/fphys.2019.00533.